

## Facile Synthesis of Hierarchically Ordered Porous Carbon via *in Situ* Self-Assembly of Colloidal Polymer and Silica Spheres and Its Use as a Catalyst Support

Shiling Zhang,<sup>†</sup> Ling Chen,<sup>†</sup> Shuxue Zhou,<sup>†</sup> Dongyuan Zhao,<sup>‡,§</sup> and Limin Wu<sup>\*,†,§</sup>

<sup>†</sup>Department of Material Science, <sup>‡</sup>Department of Chemistry, and <sup>§</sup>Advanced Materials Laboratory, Fudan University, Shanghai 200433, China

Received January 25, 2010. Revised Manuscript Received April 29, 2010

This article presents a one-pot method to synthesize hierarchically ordered porous carbons with interconnected macropores and mesopores, via *in situ* self-assembly of colloidal polymer and silica spheres with sucrose as the carbon source. Compared with other techniques, this procedure is veritably simple; neither presynthesis of the macropore/mesopore or crystal templates nor additional infiltration is needed, and the self-assembly of polymer spheres into the crystal template and the infiltration are finished *in situ* in the same system. The sizes of macropores and mesopores can be independently tuned by the sizes of polymer and silica spheres, respectively. The obtained bimodal porous carbons have large BET surface areas, large pore volumes, and partially graphitized frameworks. They show very good support of the Pt–Ru alloy catalyst in a direct methanol fuel cell.

### Introduction

Ordered porous carbon materials with tunable pore geometry and functionality have received a great deal of attention due to their many applications, such as electrode materials for batteries, fuel cells, and supercapacitors,<sup>1–3</sup> sorbents,<sup>4</sup> supports for many important catalytic processes,<sup>5</sup> templates for the preparation of other nanostructured inorganic materials,<sup>6,7</sup> photonic waveguides,<sup>8,9</sup> and so on.<sup>10,11</sup> Such diverse applications are directly related not only to their superior physical and chemical properties, such as good electric conductivity, high thermal conductivity, chemical stability, high surface area, tailorable surface properties, and low density, but also to their wide availability.

Up to now, a variety of approaches have been developed for the preparation of ordered micropore, mesopore, or macropore carbons as reviewed by Hyeon,<sup>12</sup> Ryoo,<sup>13</sup> and Stein.<sup>14</sup> For example, by using zeolites as templates, researchers successfully synthesized three-dimensional (3D) ordered microporous carbon materials with uniform pores using various carbon precursors via infiltration and chemical vapor deposition (CVD).<sup>15,16</sup> Through a nanocasting approach combined with various ordered mesopore silica as templates<sup>17,18</sup> or a direct templating preparation using supermolecular aggregates as templates, ordered mesopore carbons with different pore sizes and structures have been successfully synthesized.<sup>3,13,19–21</sup> By using inverse silica opal or colloidal crystals of polystyrene microspheres as templates, 3D ordered macropore carbons could

\*To whom correspondence should be addressed. E-mail: lmw@fudan.edu.cn.

- (1) Zhou, H.; Zhu, S.; Hibino, M.; Honma, I.; Ichihara, M. *Adv. Mater.* **2003**, *15*, 2107–2111.
- (2) Chang, H.; S. Joo, H.; Pak, C. *J. Mater. Chem.* **2007**, *17*, 3078–3088.
- (3) Liu, H. J.; Cui, W. J.; Jin, L. H.; Wang, C. X.; Xia, Y. Y. *J. Mater. Chem.* **2009**, *19*, 3661–3667.
- (4) Fang, B.; Zhou, H.; Honma, I. *J. Phys. Chem. B* **2006**, *110*, 4875–4880.
- (5) Yu, J. S.; Kang, S.; Yoon, S. B.; Chai, G. *J. Am. Chem. Soc.* **2002**, *124*, 9382–9383.
- (6) Kim, J. Y.; Yoon, S. B.; Yu, J. S. *Chem. Mater.* **2003**, *15*, 1932–1934.
- (7) Dibandjo, P.; Bois, L.; Chassagneux, F.; Cornu, D.; Letoffe, J.; Toury, B.; Babonneau, F.; Miele, P. *Adv. Mater.* **2005**, *17*, 571–574.
- (8) Zakhidov, A. A.; Baughman, R. H.; Iqbal, Z.; Cui, C. X.; Khayrullin, I.; Dantas, S. O.; Marti, J.; Ralchenko, V. G. *Science* **1998**, *282*, 897–901.
- (9) Li, H.; Chang, L.; Wang, J.; Yang, L.; Song, Y. *J. Mater. Chem.* **2008**, *18*, 5098–5103.
- (10) Yoo, W. C.; Kumar, S.; Wang, Z.; Ergang, N. S.; Fan, W.; Karanikolos, G. N.; McCormick, A. V.; Penn, R. L.; Tsapatsis, M.; Stein, A. *Angew. Chem., Int. Ed.* **2008**, *47*, 9096–9099.
- (11) Kyotani, T. *Carbon* **2000**, *38*, 269–286.

- (12) Lee, J.; Kim, J.; Hyeon, T. *Adv. Mater.* **2006**, *18*, 2073–2094.
- (13) Ryoo, R.; Joo, S. H.; Kruk, M.; Jaroniec, M. *Adv. Mater.* **2001**, *13*, 677–681.
- (14) Stein, A.; Wang, Z.; Fierke, M. A. *Adv. Mater.* **2009**, *21*, 265–293.
- (15) Hou, P.; Orikasa, H.; Yamazaki, T.; Matsuoka, K.; Tomita, A.; Setoyama, N.; Fukushima, Y.; Kyotani, T. *Chem. Mater.* **2005**, *17*, 5187–5193.
- (16) Ma, Z.; Kyotani, T.; Tomita, A. *Chem. Commun.* **2000**, 2365–2366.
- (17) Lu, A.; Kiefer, A.; Schmidt, W.; Schüth, F. *Chem. Mater.* **2004**, *16*, 100–103.
- (18) Joo, S. H.; Choi, S. J.; Oh, I.; Kwak, J.; Liu, Z.; Terasaki, O.; Ryoo, R. *Nature* **2001**, *412*, 169–172.
- (19) Deng, Y.; Yu, T.; Wan, Y.; Shi, Y.; Meng, Y.; Gu, D.; Zhang, L.; Huang, Y.; Liu, C.; Wu, X.; Zhao, D. *J. Am. Chem. Soc.* **2007**, *129*, 1690–1697.
- (20) Kosonen, H.; Valkama, S.; Nykänen, A.; Toivanen, M.; Brinke, G. T.; Ruokolainen, J.; Ikkala, O. *Adv. Mater.* **2006**, *18*, 201–205.
- (21) Liang, C.; Hong, K.; Guiochon, G. A.; Mays, J. W.; Dai, S. *Angew. Chem., Int. Ed.* **2004**, *43*, 5785–5789.

also be successfully synthesized through infiltration or CVD.<sup>5,8,9,22–28</sup>

Recently, much attention has been paid to prepare hierarchically ordered porous carbon materials, especially those possessing well-defined macropores and interconnected micropores and/or mesopores, because this bimodal porous structure can provide highly efficient mass transport through the macropores and high surface areas from micro/mesopores, as well as selective accessibility of various sizes of species. For example, Stein et al.<sup>29</sup> and Yu et al.<sup>30,31</sup> successfully prepared bimodal porous carbons by a multi-step templating method. First, 3D ordered bimodal porous silica was prepared when polymer crystals were used as templates and then calcinated; then, the ordered bimodal porous silica was infiltrated with carbon precursors; and the composites were finally calcinated and subsequently etched to achieve hierarchically ordered porous carbons. Kanamura et al.<sup>32</sup> reported the synthesis of bimodal carbons using polystyrene (PS) spheres and silica particles as templates, and PS also served as the carbon source. Zhao et al.<sup>33</sup> successfully prepared ordered bimodal porous carbon structures by the dual colloidal crystal/block copolymer template approach. First, the large and monodisperse silica microspheres (typically several hundred nanometers) self-assembled into 3D crystal array by sedimentation, followed by solvent evaporation and thermal treatment. Second, the silica colloidal crystal was used as a template and impregnated with an amphiphilic triblock copolymer and phenolic resol precursors solution, which self-organized during the evaporation of the solvent and thermosetting of phenolic resol. The composite was finally carbonized and treated with HF solution to achieve hierarchically ordered porous carbons. The large silica hard template and triblock copolymer soft template were responsible for the formation of macropores and mesopores, respectively.

Unfortunately, although the above pioneering works are very interesting, the preparation procedure, which includes presynthesis of ordered porous silica or crystals as templates, infiltration, carbonization and dissolution, seem to be time-consuming and arduous, and the mesopore size of the obtained carbon materials is either too

small or untunable. These disadvantages severely limit their practical applications. Herein, we report, for the first time, a novel and simple method we call an *in situ* self-assembly strategy of colloidal polymer and silica spheres to prepare hierarchically ordered porous carbons with interconnected macropores and mesopores. In this approach, colloidal polymer spheres are first blended with colloidal silica and then with sucrose and sulfuric acid to obtain stable dispersion. When this dispersion is cast on a glass substrate and treated at different temperatures, followed by etching in HF solution to remove silica, a hierarchically ordered porous carbon can be directly yielded. In comparison with previous techniques, our *in situ* self-assembly approach at least has the following merits: (i) the synthetic procedure is veritably quite simple, neither presynthesis of the macropore/mesopore or crystal templates nor additional infiltration is needed, and both the self-assembly of polymer spheres into the crystal template and the infiltration are finished *in situ* in the same system; (ii) the macropore and mesopore sizes can be easily tuned by changing polymer and silica particles in diameter, respectively, and the mesopore size can be modulated in the whole mesopore range (2–50 nm); (iii) soft polymer spheres ( $T_g = 21\text{ }^\circ\text{C}$ ) rather than hard PS spheres are used, this can prepare intermediate composite films (not powder), and sulfuric acid is added into the stable dispersion as the carbonization catalyst, which makes carbonization occur at a relatively lower temperature; (iv) this approach is mild and can be used for the mass of production of hierarchically ordered porous carbon. Preliminary research shows that this bimodal porous carbon as supports can significantly increase the catalytic activity of the Pt–Ru catalyst.

## Experimental Section

**Materials.** Methyl methacrylate (MMA), butyl acrylate (BA), acrylic acid (AA), and sucrose ( $T_m = 185\text{ }^\circ\text{C}$ ) were purchased from Sinopharm Chemical Reagent Corp. Auxiliary monomers: allyloxy hydroxypropyl sodium sulfonate (HAPS, 40 wt % of solid content in aqueous solution) was kindly donated by Shuangjian Trading Corp. Ltd. (China). The initiator, ammonium persulfate (APS), was obtained from Shanghai Guanghua Chemical Reagent Corp. (China). Colloidal silica: R1050 (50 nm, pH 9, solid content of 50 wt %, and zeta potential of  $-43.5\text{ mV}$ ) was provided by Eka Chemicals Corp. (Sweden), Snowtex 50 (20 nm, pH 10, solid content of 50 wt %, and zeta potential of  $-48.0\text{ mV}$ ) was obtained from Nissan Chemicals (Japan), and Nexsil 8 (9 nm, pH 10, solid content of 30 wt %, and zeta potential of  $-47.1\text{ mV}$ ) was supplied by Nyacol Nanotechnologies, Inc. (USA).  $\text{H}_2\text{PtCl}_6 \cdot 6\text{H}_2\text{O}$  and  $\text{RuCl}_3$  were purchased from Aldrich. Nafion (10 wt %) was provided by DuPont company. Commercially available 30 wt % Pt–Ru/C (weight ratio Pt/Ru = 2:1) catalyst was purchased from E-TEK Inc.

**Synthesis of Colloidal Polymer Spheres.** P(MMA-BA-AA) copolymer latex was synthesized by semibatch surfactant-free emulsion polymerization.<sup>34</sup> The size of polymer spheres could be adjusted by the amount of monomers. Three kinds of polymer latex with sizes of 475, 370, and 280 nm were obtained. The glass transition temperature of the polymer was about  $21\text{ }^\circ\text{C}$ .

- (22) Lee, K. T.; Lytle, J. C.; Ergang, N. S.; Oh, S. M.; Stein, A. *Adv. Funct. Mater.* **2005**, *15*, 547–556.
- (23) Lei, Z.; Zhang, Y.; Wang, H.; Ke, Y.; Li, J.; Li, F.; Xing, J. *J. Mater. Chem.* **2001**, *11*, 1975–1977.
- (24) Zhou, Z.; Yan, Q.; Su, F.; Zhao, X. *J. Mater. Chem.* **2005**, *15*, 2569–2574.
- (25) Chai, G. S.; Yoon, S. B.; Yu, J. S.; Choi, J. H.; Sung, Y. E. *J. Phys. Chem. B* **2004**, *108*, 7074–7079.
- (26) Su, F.; Zhao, X.; Wang, Y.; Zeng, J.; Zhou, Z.; Lee, J. Y. *J. Phys. Chem. B* **2005**, *109*, 20200–20206.
- (27) Yoon, S. B.; Chai, G. S.; Kang, S. K.; Yu, J. S.; Gierszal, K. P.; Jaroniec, M. *J. Am. Chem. Soc.* **2005**, *127*, 4188–4189.
- (28) Baumann, T. F.; Satcher, J. H., Jr. *Chem. Mater.* **2003**, *15*, 3745–3747.
- (29) Wang, Z.; Li, F.; Ergang, N. S.; Stein, A. *Chem. Mater.* **2006**, *18*, 5543–5553.
- (30) Chai, G. S.; Shin, S.; Yu, J. S. *Adv. Mater.* **2004**, *16*, 2057–2061.
- (31) Fang, B.; Kim, J. H.; Kim, M.; Yu, J. S. *Chem. Mater.* **2009**, *21*, 789–796.
- (32) Woo, S. W.; Dokko, K.; Nakano, H.; Kanamura, K. *J. Mater. Chem.* **2008**, *18*, 1674–1680.
- (33) Deng, Y.; Liu, C.; Yu, T.; Liu, F.; Zhang, F.; Wan, Y.; Zhang, L.; Wang, C.; Tu, B.; Webley, P. A.; Wang, H.; Zhao, D. *Chem. Mater.* **2007**, *19*, 3271–3277.

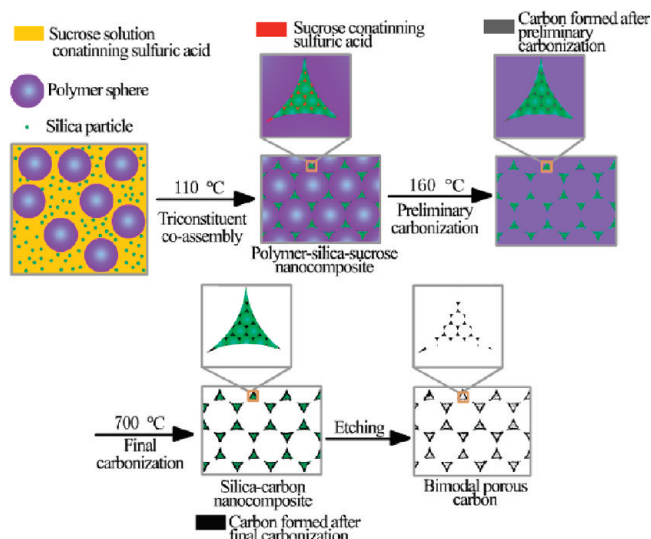
- (34) You, B.; Wen, N.; Shi, L.; Wu, L.; Zi, J. *J. Mater. Chem.* **2009**, *19*, 3594–3597.

**Preparation of Hierarchically Ordered Porous Carbons.** The hierarchically ordered porous carbons were prepared through an *in situ* self-assembly approach of colloidal polymer spheres and silica particles. For a typical procedure, 20 g of the polymer latex was first blended with 1.3 g of silica sol under magnetic stirring for 1 h to obtain nanocomposite latex and then with 0.45 g of sucrose powder at room temperature for 10 min, followed by the addition of 0.45 g of 10 wt % of sulfuric acid and 0.1 g of water under stirring for another 10 min to obtain stable dispersion; the polymer solid content of dispersion was modulated with water to 15 wt %. The typical mass ratio of polymer, silica, sucrose, and sulfuric acid was 100:15:15:1.5. The as-prepared dispersion was cast on glass substrates by the pouring method and directly dried in an oven at 110 °C for 2 h, then at 160 °C for 6 h, followed by heating to 700 °C with a rate of 5 °C/min under highly pure nitrogen flow (1 L/min), and kept at 700 °C for another 2 h to decompose polymer spheres and carbonize sucrose. The obtained carbon/silica composite was cooled in pure nitrogen and immersed in 10 wt % of HF aqueous solution to remove silica (hazard: HF is highly toxic and corrosive and must be handled in fume hoods with proper personal protection equipment), followed by washing with deionized water and drying at 60 °C to yield hierarchically ordered porous carbons.

**Carbon Supported Pt–Ru catalyst.** The carbon supported Pt–Ru catalyst was prepared by a borohydride reduction method.<sup>5</sup> The metal loading was kept at 30 wt % (weight ratio Pt/Ru = 2:1) to allow a comparison with a commercial catalyst, which was also confirmed by TGA and EDX measurements. The thin film electrode used as the work electrode in the electrochemical measurement was manufactured as follows:<sup>35</sup> 50 mg of porous carbon supported Pt–Ru catalyst powder and 250  $\mu$ L of Nafion (10 wt %) were ultrasonically dispersed in 10 mL of isopropanol. A 100  $\mu$ L portion of the resultant ink was dropped onto an electrode surface. Then, the electrode was dried at 70 °C. The cyclic voltammograms measurements in the 0.5 M  $\text{H}_2\text{SO}_4$ +1.0 M  $\text{CH}_3\text{OH}$  solution was carried out in a potentiostat of ECO CHEMIE B. V Model T30/FRA2, and a Pt sheet and saturated calomel electrodes were used as the counter and reference electrodes, respectively. The potential scan was carried out between 0.05 and 0.75 V with a scan rate of 10 mV s<sup>-1</sup> under a temperature of 40 °C.

**Characterization.** SEM was conducted with a Philips XL 30 field emission microscope at an accelerating voltage of 10 kV. High-resolution SEM (HR-SEM) was conducted on a Hitachi S-4800 microscope (Japan) operated at 1.0 kV. Transmission electron microscopy (TEM) images were taken with a JEOL 2011 microscope (Japan) operating at 200 kV. For the TEM observations, the samples were dispersed in ethanol and then dried on a holey carbon film Cu grid.  $\text{N}_2$  adsorption–desorption isotherms were measured at 77 K on a Micromeritics ASAP 2020 gas sorptometer (USA) after the carbon and carbon/silica composite was degassed at 423 K to 20  $\mu$ Torr for 12 h. The specific surface areas were determined from nitrogen adsorption using the Brunauer–Emmett–Teller (BET) equation. By using the Barret–Joyner–Halenda (BJH) model, the pore volumes and pore size distributions were derived from the adsorption branches of isotherms, and the total pore volumes were estimated from the adsorbed amount at a relative pressure  $P/P_0$  of 0.992. Raman spectra were obtained with a Dilor LabRam-1B microscopic Raman spectrometer (France), using a He–Ne laser with an excitation wavelength of 632.8 nm. XRD measurement was carried out with a Rigaku D/max-rB X-ray diffractometer with

**Scheme 1. Schematic Illustration for the Preparation of Hierarchically Ordered Porous Carbon**



Cu K $\alpha$  radiation ( $\lambda = 1.54056 \text{ \AA}$ ) at a scanning rate of 0.02° per second at  $2\theta$  ranging from 5 to 60°.

## Results and discussion

**Preparation of the Hierarchically Ordered Porous Carbon.** The hierarchically ordered porous carbons were prepared via an *in situ* self-assembly of colloidal polymer and silica spheres with sucrose as the carbon source and sulfuric acid as the catalyst, as schematically described in Scheme 1. First, colloidal poly(MMA-BA-AA) spheres were blended with colloidal silica, followed by sucrose and sulfuric acid to obtain stable dispersion. This dispersion was then cast on a glass substrate and directly dried in an oven at 110 °C for 2 h to cause a transparent film, followed at 160 °C for 6 h for preliminary carbonization by sulfuric acid to obtain black composite films, and then fully carbonized at 700 °C in  $\text{N}_2$  for another 2 h to yield iridescent black silica/carbon composite films after the decomposition of polymer spheres and sucrose. The obtained silica/carbon composite was finally etched by HF solution to remove silica to directly form iridescent black hierarchically ordered porous carbon.

The typical cross-sectional SEM images of the treated composite by different temperatures are demonstrated in Figure 1. After treatment at 110 and 160 °C, although an individual polymer sphere is not visible due to high drying temperatures, the periodic arrangement of these spheres can still be observed (Figure 1a and b). Since soft polymer spheres ( $T_g = 21 \text{ °C}$ ) rather than hard PS or PMMA spheres were used as the template, on the one hand, small silica particles occupied the interstitial voids between large polymer spheres; on the other hand, sucrose molecules and some of the polymer chains could easily diffuse and reversely fill the remaining free volumes among the silica particles. This availed the connection of neighboring macropores, greatly shortening the preparation time, and the robust intermediate composite films (not powder; Figure S1 in Supporting Information) were

(35) Chen, L.; Guo, M.; Zhang, H.; Wang, X. *Electrochim. Acta* **2006**, 52, 1191–1198.



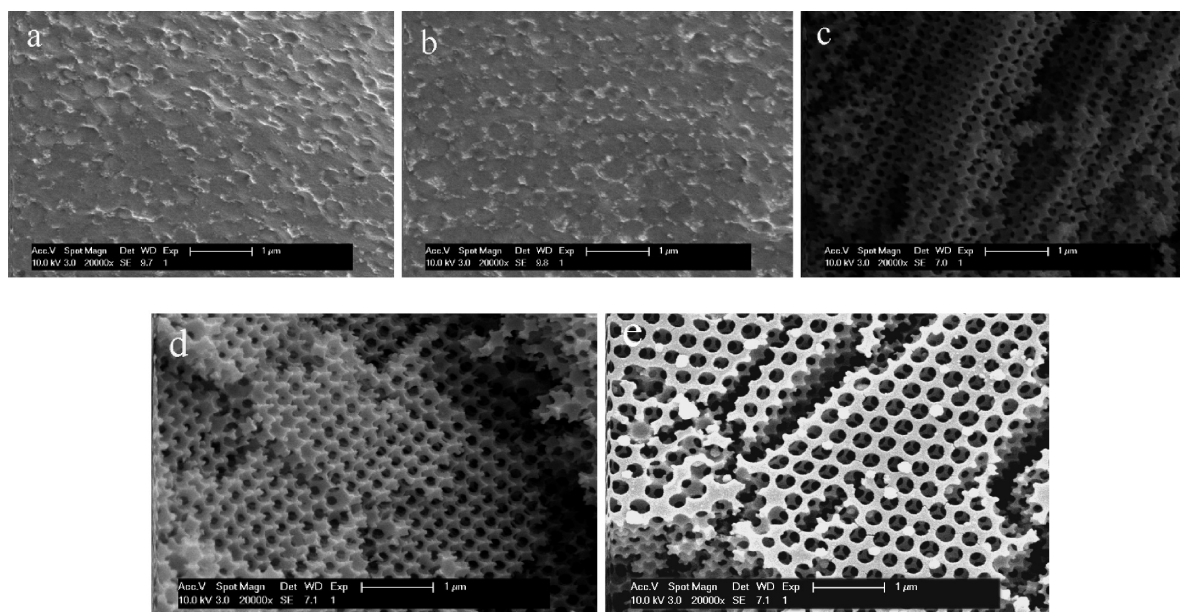


**Figure 1.** Typical cross-sectional SEM images of (a) composite films treated at 110 °C, (b) composite films treated at 160 °C, (c) porous silica/carbon composite film, (d) bimodal porous carbon, and (e) surface SEM image of bimodal porous carbon (polymer spheres, 370 nm; silica colloid, 9 nm; sucrose, 15 wt %; silica, 15 wt %).

also in favor of the mass production of bimodal porous carbons. Furthermore, the surrounding nanosilica particles and sucrose crystallites could restrain the deformation and coalescence of these soft polymer spheres, which could guarantee these monodisperse and spherical polymer spheres to tightly pile into 3D ordered arrays.<sup>34</sup> The results are also consistent with previous works using viscous liquids.<sup>36,37</sup> After being completely carbonized, the obtained silica/carbon composite reveals a 3D ordered porous structure (Figure 1c). The macropore size estimated from SEM is about 350 nm, around 5% of shrinkage of the lattice structure compared to that of polymer spheres. These 3D ordered macropores are connecting each other by small windows with a size of 120 nm that are caused by the contacting area between neighboring polymer spheres. After the removal of silica microspheres, the product also presents 3D interconnection of the ordered macropores with small windows, indicating that the macrostructure of the colloidal polymer crystals can be well retained (Figure 1d). Moreover, this structure appears to be typical face-centered cubic (fcc), which can be observed in the (100) plane in Figure 1d, with each pore surrounded by six equal pores in layers perpendicular to the (111) direction (Figure 1e).

**Effects of Silica and Polymer Sizes.** Figure 2 displays the cross-sectional SEM and HRTEM images of 3D ordered porous carbons prepared from different sizes of silica. The inserted HRSEM images in Figure 2a–c clearly reveal that the macropores are interconnected by windows and that the pore walls are composed of spherical mesopores. The HRTEM images in Figure 2d and e also show mesopores between macropores, indicating a

hierarchically ordered porous structure. Moreover, the mesopore size increases from about 9 to 50 nm with the increase of colloidal silica size from around 9 to 50 nm, indicating that the mesopore size can be easily and independently adjusted in the full mesopore range by the size of silica particles. This cannot be easily realized in other templating approaches.<sup>29–31,33</sup>

When the polymer spheres with a size of 280 or 475 nm were used, this hierarchically ordered porous carbon could also be prepared, as indicated in Figure 3. These results show that the higher ratio of small nanoparticles to large sphere sizes than the theoretical 0.155 can also form an organization arrangement,<sup>38</sup> which is consistent with a previous report.<sup>39</sup> This is probably because some polymer chains of the soft polymer spheres in our system could contrarily diffuse into the voids between silica particles as the dispersion was dried at 110 °C, causing a ratio higher than the theoretical value.

**Effects of Silica and Sucrose Contents.** When too low of an amount of silica, i.e., 5 wt %, was used, a collapsing skeleton was observed (Figure 4a), while the windows were dramatically decreased in size, even closed completely, when too much silica, i.e., 35 wt %, was embedded (Figure 4b). If the amount of silica further increased to 40 wt %, a mesopore domain formed due to the silica domain (Figure 4c). This suggests that the efficient infiltration of silica into the voids between polymer spheres is playing a critical role for the successful preparation of hierarchically ordered porous carbon structures in our *in situ* self-assembly approach: too low an amount of silica is not enough for the formation of an integrated silica framework, but excess silica would impede the contact of neighboring polymer spheres except for filling in the voids between polymer spheres and even

(36) Kim, S. H.; Kim, S. H.; Yang, S. M. *Adv. Mater.* **2009**, *21*, 3771–3775.

(37) Jiang, P.; McFarland, M. J. *J. Am. Chem. Soc.* **2004**, *126*, 13778–13786.

(38) Iskandar, F.; Mikrajuddin; Okuyama, K. *Nano Lett.* **2002**, *2*, 389.

(39) Wang, J.; Li, Q.; Knoll, W.; Jonas, U. *J. Am. Chem. Soc.* **2006**, *128*, 15606–15607.

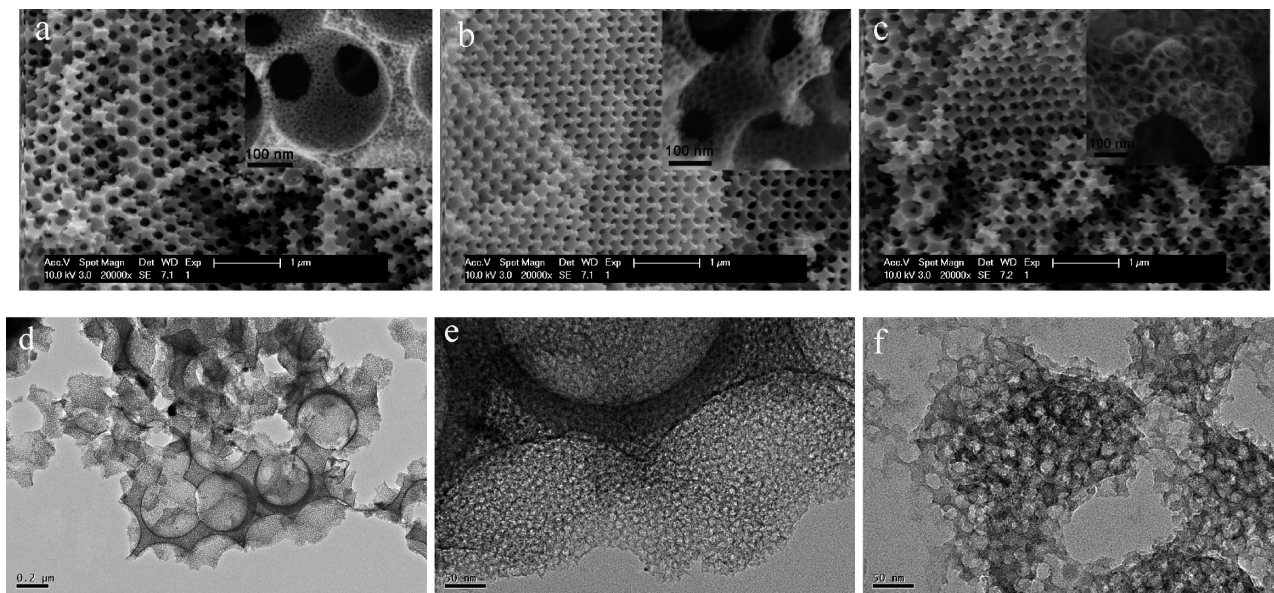


**Figure 2.** Typical cross-sectional SEM and HRTEM images of the bimodal porous carbons prepared from different sizes of silica. (a, d, and e) 9 nm, (b) and f) 20 nm, and (c) 50 nm (bar in HRTEM images: d is 200 nm; bars in e and f are 50 nm; insets are corresponding HRSEM images for macropore wall, and all bars are 100 nm; polymer sphere size is 370 nm).

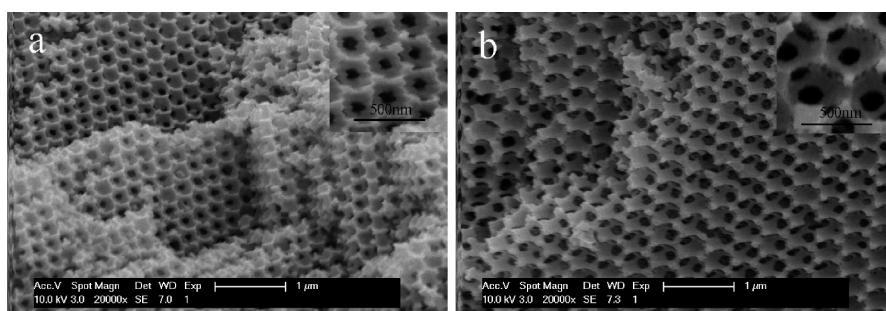


**Figure 3.** Cross-sectional SEM images of the porous carbon films prepared from (a) 280 nm polymer spheres, (b) 475 nm polymer spheres (inserts are corresponding amplified SEM image; silica particle size is 9 nm).

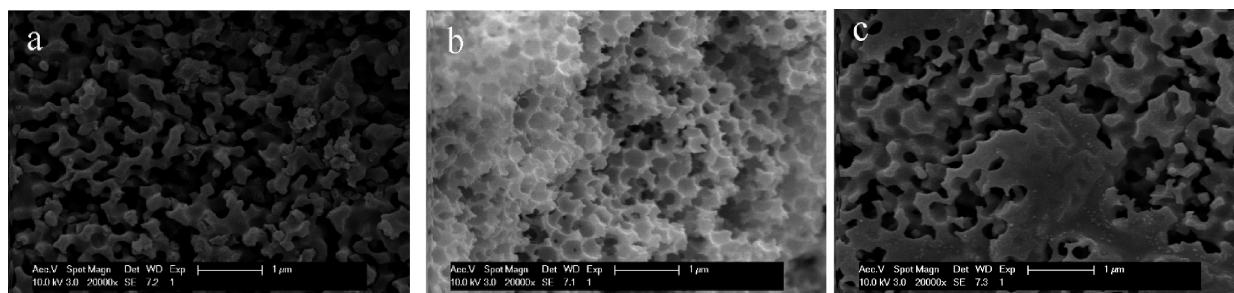


**Figure 4.** Cross-sectional SEM images of the porous carbon films prepared from different amounts of silica: (a) 5 wt %, (b) 35 wt %, and (c) 40 wt % (the sizes of polymer and silica particles are 370 and 9 nm, respectively).

form a silica domain. On the basis of the above results, 15 wt % of silica is appropriate for the formation of an ordered porous structure.

When 5 or 15 wt % of sucrose was used, hierarchically ordered porous carbons with interconnected macropores and mesopores could also be obtained, as indicated by Figure 5. But excess sucrose crystallites would cumber the osculation of neighboring polymer spheres, leading to closed windows, just as excess silica does.

**Adsorption and XRD Analyses.** Figure 6 demonstrates the typical nitrogen adsorption–desorption isotherms at

77 K and the pore size distributions of hierarchically ordered porous carbons. The corresponding pore sizes, BET surface areas, and pore volumes are summarized in Table 1. All these ordered porous carbons display type IV isotherms with a H2 hysteresis, which is the characteristic of mesopores. The carbons prepared from 280, 370, and 475 nm polymer spheres and 9 nm silica have a calculated pore size of approximately 9 nm from the adsorption branch by the BJH model (inset of Figure 6a), and almost equal BET surface areas and pore volumes, with as high as 781, 818, and 765 m<sup>2</sup>/g, and 1.23, 1.29, and 1.22 cm<sup>3</sup> STP/g,



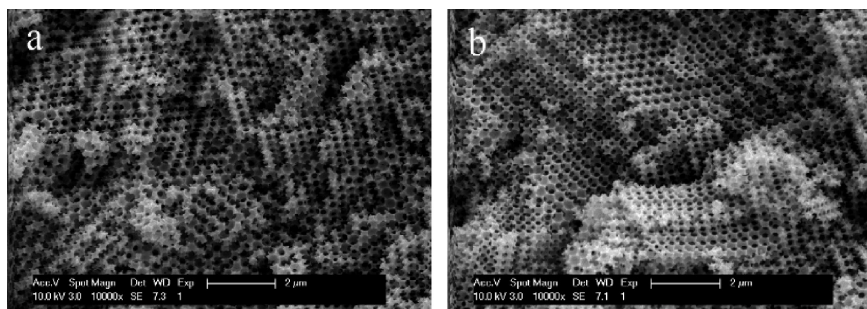


**Figure 5.** Cross-sectional SEM images of the porous carbons prepared from different sucrose content: (a) 5 wt %; (b) 15 wt % (polymer spheres, 370 nm; silica, 15 wt %).

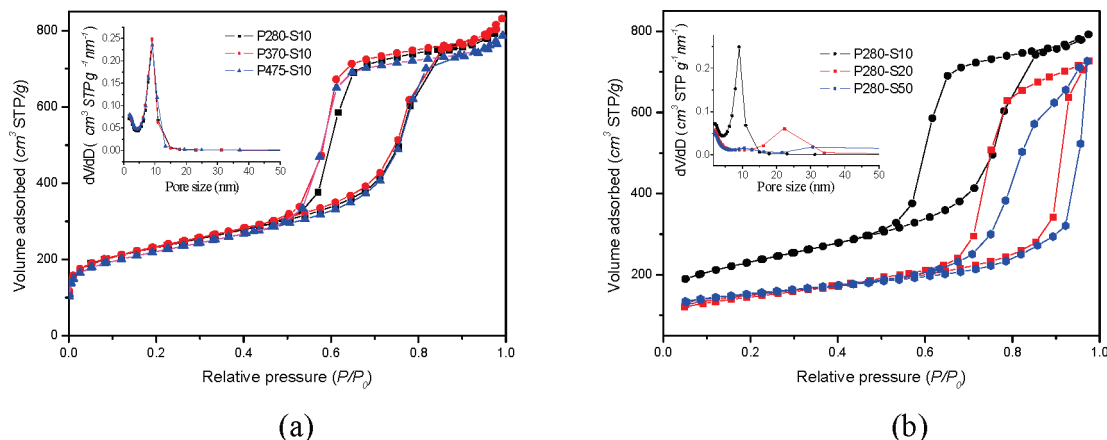


**Figure 6.** Typical  $N_2$  adsorption isotherms and pore size distribution (inset) of some ordered bimodal porous carbons (a) from different sizes of polymer spheres; (b) from different sizes of silica (P280, P370, and P475 denote polymer spheres with sizes of 280, 370, and 475 nm, respectively; S9, S20 and S50 denote silica beads with sizes of 9, 20, and 50 nm, respectively).

**Table 1. Structural Parameters of Porous Silica/Carbon Composite, Silica, and Carbon<sup>a</sup>**

sample <sup>a</sup>	macropore size (nm) <sup>c</sup>	mesopore diameter (nm) <sup>d</sup>	BET surface area (m <sup>2</sup> g <sup>-1</sup> )	total pore volume (cm <sup>3</sup> STP g <sup>-1</sup> )	micropore volume (cm <sup>3</sup> STP g <sup>-1</sup> )
P280-S9 composite	260		98	0.084	0.034
P280-S9 silica	260		204	0.33	0.00
P280-S9-0.05 <sup>b</sup>	260	9.0	850	1.61	0.04
P280-S9	260	9.0	781	1.23	0.11
P280-S20	260	22.2	509	1.12	0.09
P280-S50	260	50.0 <sup>c</sup>	527	1.12	0.12
P370-S9	350	9.0	818	1.29	0.11
P475-S9	440	9.0	765	1.22	0.10

<sup>a</sup> Both silica and sucrose contents: 15 wt %. <sup>b</sup> Silica content, 15 wt %; sucrose content, 5 wt %. <sup>c</sup> By SEM images. <sup>d</sup> From the PSD max.

respectively (Table 1), which are comparable with those from these approaches of presynthesizing templates.<sup>29–33</sup> These results indicate that the sizes of polymer spheres have little impact on the BET surface area and the pore volume. However, as sucrose content decreases from 15 to 5 wt %, the surface area and total pore volume increase from 781 to 850.1 m<sup>2</sup>/g, and from 1.23 to 1.61 cm<sup>3</sup> STP/g, respectively, indicating that both of them can be tuned by sucrose content.

For the carbons prepared from silica with a size of 9, 20, and 50 nm, the capillary condensation steps shift to low relative pressure when the mesopore size decreases from 50 to 9 nm (Figure 6b). The samples from 9 and 20 nm silica have pore sizes of 9 and 22 nm (inset of Figure 6b), which are consistent with the sizes of silica beads used. However, the sample from 50 nm silica possesses a wider mesopore

distribution in the whole mesopore region. This is probably attributed to the increasing interstices between hollow carbon spheres and the windows connecting mesosized carbon spheres besides mesopores. The specific surface area decreases from 781 and 509 to 527 m<sup>2</sup>/g, while pore volume is not varied when the size of silica increases from 9 and 20 to 50 nm, indicating that the specific surface area can also be controlled by the size of the silica beads used.

The Raman spectrum (Figure 7) shows two strong broad bands at 1320 and 1585 cm<sup>-1</sup> that can be assigned to the D and G bands of the disordered and graphitized carbons, respectively. Considering that the G band is associated with graphitic sp<sup>2</sup> carbon structures,<sup>40</sup> the comparable intensity

(40) Sadezky, A.; Muckenhuber, H.; Grothe, H.; Niessner, R.; Poschl, U. *Carbon* **2005**, *43*, 1731–1742.

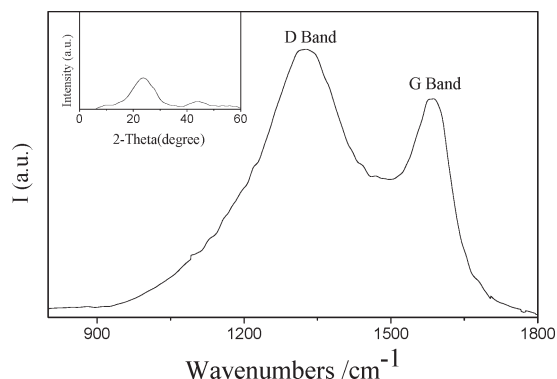


**Figure 7.** Typical Raman spectrum and XRD pattern (inset) of the bimodal porous carbon.

of D and G bands (the intensity ratio,  $\sim 1.22$ ) suggests that the hierarchically ordered porous carbon materials are partially composed of graphites. The XRD pattern (inset of Figure 7) shows two broad reflections at  $2\theta$  of ca. 22 and 44°, which can be attributed to turbostratic packing of graphene sheets in amorphous carbon.

**Formation Mechanism of Hierarchically Ordered Porous Carbons.** On the basis of the above observations, the formation mechanism of hierarchically ordered porous carbons via the *in situ* self-assembly approach can be explained as follows: When the dispersion of colloidal polymer spheres, colloidal silica, sucrose, and sulfuric acid was cast on glass substrates and directly dried in an oven at 110 °C, the charged colloidal polymer spheres came into close contact via capillaries as water evaporated. During this *in situ* self-assembly process, the deformation and coalescence of these soft polymer spheres were restrained due to the surrounding nanosilica particles and sucrose crystallites.<sup>34</sup> This could guarantee that these monodisperse and spherical polymer spheres tightly pile into 3D ordered arrays, in which the voids were filled *in situ* with nanosilica particles as well as sucrose crystallites in the same system. When this dried transparent film was treated at 160 °C for preliminary carbonization, then at 700 °C for full carbonization, polymer spheres were removed, leaving behind macropore silica/carbon composites, which reveals a characteristic of multilayer adsorption on macropore solids. The silica in the pore walls was acting as a rigid framework to prevent large shrinkage of the pores during the pyrolytic removal of organic components. This composite was finally etched by HF solution to remove silica to form hierarchically ordered porous carbons with interconnected macropores and mesopores. The whole process neither needs the presynthesis of the macropore/mesopore or crystal templates nor additional infiltration; both the polymer crystal and the infiltration are finished *in situ* in the same system.

**As Support of the Pt–Ru Alloy Catalyst.** The obtained hierarchically ordered porous carbons were further used as the support of the Pt–Ru alloy catalyst and compared with the commercially available E-TEK catalysts with Pt–Ru alloy supported on carbon.<sup>31,41</sup> The Pt–Ru alloy catalysts

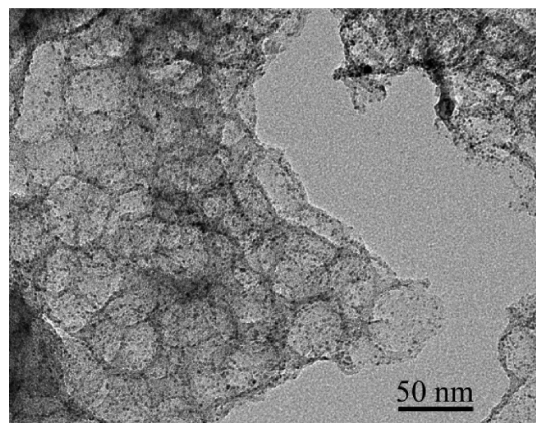


**Figure 8.** TEM image of the porous supported Pt–Ru catalyst.

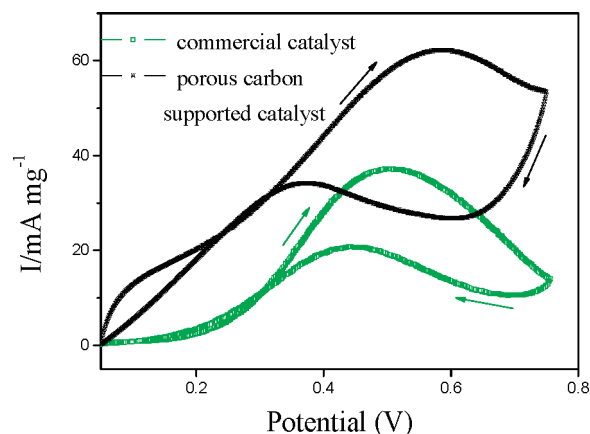


**Figure 9.** Cyclic voltammograms for a porous carbon supported Pt–Ru catalyst as compared with that of a commercial catalyst for methanol oxidation.

were prepared by the borohydride reduction method<sup>5</sup> using our porous carbon with a 350 nm macropore size and 50 nm mesopore size as a catalyst support. The TEM image of the supported catalysts show a homogeneous dispersion of Pt–Ru alloy metal particles with around 2 nm (Figure 8). The cyclic voltammograms of porous carbon supported Pt–Ru catalyst and the commercial E-TEK catalyst, as illustrated in Figure 9, display that the specific mass current density at the same potential for the porous carbon supported catalyst is considerably higher than that for the commercial catalyst in the forward as well as the reverse scan. This indicates that the Pt–Ru catalyst supported on our bimodal porous carbon has higher catalytic activity than the commercial E-TEK catalyst. This should be attributed to the higher surface and efficient diffusion of methanol and oxidized product in the 3D interconnected macropores and mesopores.

## Conclusions

On the basis of this study, a novel and feasible approach to prepare hierarchically ordered porous carbons with interconnected macropores and mesopores has been proposed via an *in situ* self-assembly approach. This is the first example of the self-assembly of soft colloidal polymer spheres and silica particles in carbon source solution

in the preparation of bimodal ordered porous carbons. The surrounding nanosilica particles and sucrose crystallites can restrain the deformation and coalescence of these soft polymer spheres, which can guarantee that these monodisperse and spherical polymer spheres tightly pile into 3D ordered arrays. Compared to previous techniques, this method neither needs the presynthesis of the macropore/mesopore silica or crystal silica as templates nor the additional infiltration, and both the self-assembly of polymer spheres into the crystal template and the infiltration are finished *in situ* in the same system. This approach is simple, mild, environmentally friendly, and can be used for the mass production of hierarchically ordered porous carbon. The macropore and mesopore sizes could be easily tuned by the sizes of polymer and silica particles, respectively.

The obtained hierarchically ordered carbons can greatly enhance the catalytic activity of catalyst as supports and could also be used as supports for titania, zirconia, tin oxide, etc., which would open new possibilities for technology applications in other application fields.

**Acknowledgment.** Financial support of this research from Shanghai-Unilever Research and Development Fund (07su07001), the NSF (No. 20774023), the Shanghai Leading Academic Discipline Project (B113), and the Shuguang Scholar-Tracking Foundation of Shanghai is appreciated.

**Supporting Information Available:** Typical optical photos of a composite film after preliminary and final carbonization, and bimodal porous carbon (PDF). This material is available free of charge via the Internet at <http://pubs.acs.org>.